

Article

# Cardio-Hepatic Interaction in Cardiac Amyloidosis

Sandra Michaela Ihne-Schubert <sup>1,2,3,4,\*</sup>, Oliver Goetze <sup>1,5,6</sup>, Felix Gerstendörfer <sup>1,2</sup>, Florian Sahiti <sup>1,7,8</sup> , Ina Schade <sup>9</sup>, Aikaterini Papagianni <sup>1,10</sup> , Caroline Morbach <sup>1,7,8</sup> , Stefan Frantz <sup>1,7,8</sup>, Hermann Einsele <sup>1,2</sup> , Stefan Knop <sup>1,2,11</sup>, Claudia Sommer <sup>1,10</sup>, Beat Müllhaupt <sup>12</sup> , Torben Schubert <sup>3,13</sup> , Stefan Störk <sup>1,7,8</sup>  and Andreas Geier <sup>1,5</sup>

- <sup>1</sup> Interdisciplinary Amyloidosis Center of Northern Bavaria, University Hospital Würzburg, 97080 Würzburg, Germany
  - <sup>2</sup> Department of Internal Medicine II, Hematology, University Hospital Würzburg, 97080 Würzburg, Germany
  - <sup>3</sup> CIRCLE—Centre for Innovation Research, Lund University, 22100 Lund, Sweden
  - <sup>4</sup> Department of Internal Medicine IV, University Hospital Gießen and Marburg, 35392 Gießen, Germany
  - <sup>5</sup> Department of Internal Medicine II, Hepatology, University Hospital Würzburg, 97080 Würzburg, Germany
  - <sup>6</sup> Department of Medicine, Universitätsklinikum Knappschafts-Krankenhaus Bochum, 44892 Bochum, Germany
  - <sup>7</sup> Comprehensive Heart Failure Center, University Hospital Würzburg, 97080 Würzburg, Germany
  - <sup>8</sup> Department of Internal Medicine I, Cardiology, University Hospital Würzburg, 97080 Würzburg, Germany
  - <sup>9</sup> Department of Thoracic Surgery and Thoracic Endoscopy, Helios Klinikum Erfurt, 99089 Erfurt, Germany
  - <sup>10</sup> Department of Neurology, University Hospital Würzburg, 97080 Würzburg, Germany
  - <sup>11</sup> Department of Internal Medicine V, Hospital Nürnberg Nord, 90419 Nürnberg, Germany
  - <sup>12</sup> Department of Gastroenterology and Hepatology, University Hospital Zurich, 8091 Zurich, Switzerland
  - <sup>13</sup> Fraunhofer Institute for Systems and Innovation Research ISI, 76139 Karlsruhe, Germany
- \* Correspondence: ihne\_s@ukw.de; Tel.: +49-931-201-44959; Fax: +49-931-201-646393

**Abstract: Background:** Congestion is associated with poor prognosis in cardiac amyloidosis (CA). The cardio-hepatic interaction and the prognostic impact of secondary liver affection by cardiac congestion in CA are poorly understood and require further characterisation. **Methods:** Participants of the amyloidosis cohort study AmyKoS at the Interdisciplinary Amyloidosis Centre of Northern Bavaria with proven transthyretin (ATTR-CA) and light chain CA (AL-CA) underwent serial work-up including laboratory tests, echocardiography, and in-depth hepatic assessment by vibration-controlled transient elastography (VCTE) and <sup>13</sup>C-methacetin breath test. **Results:** In total, 74 patients with AL-CA (n = 17), ATTR-CA (n = 26) and the controls (n = 31) were analysed. ATTR-CA patients showed decreased microsomal liver function expressed by maximal percentage of dose rate (PDR<sub>peak</sub>) related to hepatic congestion. Reduced PDR<sub>peak</sub> in AL-CA could result from altered pharmacokinetics due to changed hepatic blood flow. Liver stiffness as a combined surrogate of chronic liver damage and congestion was identified as a predictor of all-cause mortality. Statistical modelling of the cardio-hepatic interaction revealed septum thickness, NT-proBNP and PDR<sub>peak</sub> as predictors of liver stiffness in both CA subtypes; dilatation of liver veins and the fibrosis score FIB-4 were only significant for ATTR-CA. **Conclusions:** Non-invasive methods allow us to characterise CA-associated hepatic pathophysiology. Liver stiffness might be promising for risk stratification in CA.

**Keywords:** cardiac amyloidosis; <sup>13</sup>C-methacetin breath test (MBT); liver stiffness; vibration-controlled transient elastography (VTCE); PDR<sub>peak</sub>; congestion



**Citation:** Ihne-Schubert, S.M.; Goetze, O.; Gerstendörfer, F.; Sahiti, F.; Schade, I.; Papagianni, A.; Morbach, C.; Frantz, S.; Einsele, H.; Knop, S.; et al. Cardio-Hepatic Interaction in Cardiac Amyloidosis. *J. Clin. Med.* **2024**, *13*, 1440. <https://doi.org/10.3390/jcm13051440>

Academic Editors: Sophie I. Mavrogeni and Attila Nemes

Received: 27 December 2023  
Revised: 27 January 2024  
Accepted: 26 February 2024  
Published: 1 March 2024



**Copyright:** © 2024 by the authors. Licensee MDPI, Basel, Switzerland. This article is an open access article distributed under the terms and conditions of the Creative Commons Attribution (CC BY) license (<https://creativecommons.org/licenses/by/4.0/>).

## 1. Introduction

Systemic amyloidosis represents a complex multi-system disorder that is caused by the deposition of misfolded proteins in the tissue leading to organ dysfunction. The prognosis depends largely on the presence and severity of cardiac involvement [1–6]. Transthyretin (ATTR) and systemic light chain (AL) amyloidosis are the most common forms in general, as well as in the subtype of cardiac amyloidosis (CA). Mechanical and local cytotoxic effects can be found as underlying pathogenetic mechanisms in both forms [1,2]. In cardiac light chain amyloidosis (AL-CA), circulating free light chains exert additional direct cardiotoxic

effects by direct activation of a MAPK pathway as the main reason for cardiotoxicity with direct influence on NT-proBNP [7–9].

Irrespective of the subtype of CA, elevated liver function tests are common. They are, however, usually neither consequences of primary liver disorders nor hepatic amyloidosis, as hepatic involvement does not occur in ATTR in general and only in about 15% of AL amyloidosis [10]. Therefore, observed elevation of liver functional tests most likely results from cardiac congestion and is thus to be considered secondary. In the light of this, the current study aims to

- (i). Non-invasively characterise and model secondary liver affection (dynamic hepatic function and tissue elasticity) in patients with CA;
- (ii). Evaluate the diagnostic and prognostic utility of quantitative dynamic liver function tests and vibration-controlled transient elastography (VCTE) regarding mortality.

## 2. Materials and Methods

### 2.1. Study Population

The Amyloidosis Cohort Study (AmyKoS) recruits consecutive patients presenting to the Interdisciplinary Amyloidosis Center of Northern Bavaria, Würzburg, Germany, with suspected or proven amyloidosis. This study complies with the Declaration of Helsinki and received positive votes from the Medical Ethics Committee at the Julius-Maximilians-University of Würzburg (48/18). All participants provided written informed consent. For the present analysis, participants with proven cardiac and excluded hepatic AL (AL-CA), according to Gertz et al. in 2005, as well as proven cardiac ATTR amyloidosis (ATTR-CA), were identified [11]. Further, control patients from the AmyKoS stock with excluded cardiac and hepatic amyloidosis manifestations entered the analysis, ensuring an identical diagnostic work-up by the same investigators and in the same setting. The subtype-spanning approach was chosen to generate generalisable results that reflect the different pathomechanisms.

All patients underwent a serial detailed work-up, including extensive laboratory tests, standardised transthoracic echocardiography, VCTE to assess liver stiffness (in kPa) and <sup>13</sup>C-methacetin breath test (MBT) for microsomal liver function expressed by PDR<sub>peak</sub>. Laboratory parameters were obtained from routine blood analysis according to locally established standards.

The well-established fibrosis score FIB-4 was calculated according to the generally applicable formula [12–14]:

$$\text{FIB-4} = \frac{\text{age [years]} \times \text{AST} \left[\frac{\text{U}}{\text{L}}\right]}{\text{platelet count} \left[\frac{10^9}{\text{L}}\right] \times \sqrt{\text{ALT} \left[\frac{\text{U}}{\text{L}}\right]}}$$

FIB-4 was cleaned for its statistical component related to congestion by regressing the score on NT-proBNP and liver vein congestion and using the residuals from the regression as a congestion-filtered version of the score (indicated by the subscript “clean”; FIB-4<sub>clean</sub>).

Microsomal function measured by MBT over 1 h of breath sampling after ingestion of 75 mg 4'-O-<sup>13</sup>C-methacetin in a fasted state (Euriso-top, 91194 Saint-Aubin Cedex, Côte-d'Or, France; chemical purity of 99.7% and an isotopic purity of 99.1%) dissolved in 100 mL water was expressed by the maximum percentage dose rate PDR<sub>peak</sub> (%/h), since the maximum <sup>13</sup>CO<sub>2</sub> excretion is least affected by post-CYP1A2 processes, such as loss through exchange reactions, e.g., with the bicarbonate pool or integration into the skeletal system [15]. This is in line with the European guideline on indications, performance and clinical impact of <sup>13</sup>C-breath tests in adult and paediatric patients [16]. Explanations regarding the applied methods can be found in the Supplementary Materials (Table S1 [12–14,16–22]). Moreover, detailed test descriptions are given elsewhere [23].

## 2.2. Independent Reference Groups for Microsomal Liver Function

The raw data of young healthy participants and patients with chronic hepatitis C infection (mean age 46.2 years, SD 11.3 years, range 20–74 years) with low histological fibrosis stages [23] were provided by O. G. and B. M. and reanalysed regarding microsomal function within different stages of fibrosis and inflammation using  $PDR_{peak}$  as a marker of interest (for the rationale, see above). Additional reference groups were identified via PubMed search using the general keyword “methacetin breath test” [23–29]. The minimum requirements for the use as a reference group were the clear definition of the reported collective by a single underlying disorder and the specification of mean, standard deviation and the total number of patients analysed for  $PDR_{peak}$  to enable comparison with the CA patients.

## 2.3. Statistical Model Development and Analysis

Since our goal was to characterise secondary liver affection in CA, we first performed a mean value comparison of the two subtypes of amyloidosis and the control in our sample, as well as with different groups of primary liver affection (see reference groups for microsomal liver function) regarding significant differences by z-test. Furthermore, the pairwise non-parametric Spearman correlation analysis was performed, referring to the cross-sectional data set of all patients at first evaluation to obtain a first impression of the prognostic value of the different liver function tests, as well as their relation to congestion.

In the second step, we focused on the effects of congestion expressed by the surrogates NTproBNP and liver vein dilatation on the hepatic metabolic (microsomal) activity expressed by  $PDR_{peak}$  and chronic liver damage, specifically fibrosis, expressed by the lab-based score FIB-4. We used multivariate linear regression analysis for the evaluation based on the panel data set resulting from a serial work-up of patients.

As FIB-4 and  $PDR_{peak}$  are only valid surrogate parameters for parts of the pathomechanisms behind secondary liver affection, we chose liver stiffness as a clinically easily accessible and well-established summatory surrogate parameter for chronic liver damage going beyond fibrosis.

In the third step, we then specifically modelled the factors influencing liver stiffness. Based on a theoretical model, which we adapted from Müller et al. [30] to the specific situation of CA, we chose the following five parameters in the final model explaining liver stiffness: septum thickness, NT-proBNP, dilatation of liver veins,  $PDR_{peak}$  and FIB-4<sub>clean</sub>. To test the effects of these theoretically derived parameters on liver stiffness, a regression approach was employed. While principally ordinary linear regression would be feasible, one problem is that further parameters may be of relevance. We therefore decided to implement a data-driven regression model, which is able to select additional parameters depending on their explanatory power. The formula to describe the statistical model can be written as follows:

$$y_{it} = \sum_{j=1}^J x_{itj} \beta_j + \sum_{k=1}^K c_{itk} \delta_k + u_{it}$$

$y_{it}$ —log stiffness;

$x_{it}$ —core variables (septum thickness, NT-proBNP, dilatation of liver veins,  $PDR_{peak}$  and FIB-4<sub>clean</sub>);

$c_{it}$ —high-dimensional control variables;

$\beta_j$ —coefficients of the variables of interest;

$\delta_k$ —coefficients of the high-dimensional control variables;

$u_{it}$ —disturbance term;

J, K—number of variables, K can become very large.

To systematically identify the relevant control variables in our high-dimensional data set and to avoid a bias due to manual pre-regression selection of control variables, a post-cluster least absolute shrinkage and selection operator regression (LASSO), following

Belloni et al. (2016) [31], was performed based on the panel data set including all available repetitive data sets of the described patient population.

In the fourth and final step, we analysed the survival among our cohort by calculating Kaplan–Meier curves and assessed the prognostic value of liver stiffness in comparison to the other two hepatic markers FIB-4 and PDR<sub>peak</sub>, as well as established cardiac biomarkers for mortality. We used a Cox regression approach with time-varying data, which expresses the mortality risk by the hazard rate, i.e., the time-normalised risk of death as a function of key explanatory variables  $x_{it}$ :

$$h(t, x_{it}) = h_0(t) \cdot \exp(x_{it}\beta)$$

$\beta$  is a vector of associated regression parameters.  $h_0(t)$  is the unknown baseline hazard defining the baseline mortality risk if all parameters  $x_{it}$  are zero. The baseline hazard is not estimated but treated as noise in the regression. The interest then lies in estimating  $\beta$ , which determines the direction of the influence each clinical parameter has on the hazard function. For example, if for a parameter the associated element of  $\beta$  is larger than zero, the influence on the hazard function is positive. In the regressions, for interpretative convenience, we do not report the raw coefficients, but their exponentiated versions, because the exponentiated coefficients can be interpreted as hazard rates. The neutral point ( $\beta = 0$ ) is then 1 because  $\exp(0) = 1$ . Also, if an estimated hazard rate is then, for example, equal to, say, 1.05, it means that a one-unit increase in a parameter increases the mortality risk in a fixed time interval by 5%. Cox regression has a number of desirable features, which make it preferable over Full Maximum Likelihood survival models. Specifically, it is semi-parametric in the sense that it does not impose parametric functional assumptions on the baseline hazard. Results were visualised by forest plots.

All statistical analyses were performed using STATA<sup>®</sup> version 14.

### 3. Results

From November 2017 until April 2020, 74 patients with AL-CA (n = 17), ATTR-CA (n = 26) and the controls (n = 31) with, in total, 177 observations, were evaluated. The basic characterisation of the cohort is summarised in Table 1. The mean age of ATTR-CA, AL-CA and controls was  $74.9 \pm 7.2$ ,  $64.0 \pm 8.1$  and  $63.1 \pm 1.6$  years, respectively.

#### 3.1. Characterisation of the Cardiac Function within the Cohort

In total, 76.9% of patients with ATTR-CA and 71.4% of those with AL-CA presented in NYHA functional class II or higher compared to 41.9% of the control patients. AL-CA and ATTR-CA patients showed the typical clinical picture of heart failure with preserved ejection fraction (HFpEF), but LVEF among ATTR-CA was significantly lower compared to AL-CA and controls within the established range for HFpEF of LVEF  $\geq 50\%$ . Septum and posterior wall thickness were significantly increased in CA, in ATTR-CA more than in AL-CA. Cardiac biomarker levels such as NT-proBNP and high-sensitive troponin T levels were also significantly elevated in both, but in AL-CA more than ATTR-CA. Diastolic function was significantly impaired in CA compared to the controls. Signs of hypervolemia were highly prevalent in CA (Tables 1 and S2). The median daily dosage of diuretics among those treated with diuretics was equivalent to 17.5 (10.0; 20.0) mg torasemide among ATTR-CA, 30.0 (16.25; 55.00) mg among AL-CA and 12.5 (9.38; 16.25) mg among controls, respectively. More details are summarised in Tables 1 and S2.

**Table 1.** Basic characterisation of the cohort.

		ATTR-CA				AL-CA				Control				ATTR-CA vs. Control		AL-CA vs. Control		ATTR-CA vs. AL-CA	
n patients		26				17				31									
n observations		60				52				65									
		<i>n</i>	<i>mean</i>	$\pm$	<i>SD</i>	<i>n</i>	<i>mean</i>	$\pm$	<i>SD</i>	<i>n</i>	<i>mean</i>	$\pm$	<i>SD</i>	<i>z</i>	<i>p value</i>	<i>z</i>	<i>p value</i>	<i>z</i>	<i>p value</i>
age [years]		26	74.9	$\pm$	7.2	17	64.0	$\pm$	8.1	31	63.1	$\pm$	11.6	4.6781	***	0.3162	n.s.	4.500	***
sex	<i>male</i>	26	84.6%			17	41.2%			31	54.8%								
	<i>female</i>	26	15.4%			17	58.8%			31	45.2%								
ECOG		26	0.5	$\pm$	0.5	16	0.5	$\pm$	0.7	30	0.2	$\pm$	0.5	2.0418	*	1.5588	n.s.	−0.061	n.s.
cardiac comorbidity		26	76.9%	$\pm$	43.0%	17	52.9%	$\pm$	51.4%	31	45.2%	$\pm$	50.6%	2.5631	*	0.5040	n.s.	1.593	n.s.
hepatic comorbidity		26	19.2%	$\pm$	40.2%	16	12.5%	$\pm$	34.2%	31	22.6%	$\pm$	42.5%	−0.3053	n.s.	−0.8801	n.s.	0.579	n.s.
number of involved organs by amyloidosis		26	1.6	$\pm$	0.5	17	2.0	$\pm$	1.3	31	1.2	$\pm$	0.5	2.7619	**	2.4877	*	−1.303	n.s.
severity of cardiac amyloidosis #	<i>stage I</i>	15	58%			1	6%												
	<i>stage II</i>	8	31%			5	29%												
	<i>stage III</i>	3	12%			11	65%												
NYHA	<i>I</i>	6	23.1%			6	28.6%			18	58.1%								
	<i>II</i>	8	30.8%			8	38.1%			9	29.0%								
	<i>III</i>	12	46.2%			6	28.6%			4	12.9%								
	<i>IV</i>	0	0.0%			1	4.8%			0	0.0%								
rhythm	<i>sinus rhythm</i>	26	53.8%	$\pm$	50.8%	17	82.4%	$\pm$	39.3%	31	90.3%	$\pm$	30.1%	−3.2173	**	−0.7276	n.s.	−2.067	*
	<i>atrial fibrillation</i>	26	38.5%	$\pm$	49.6%	17	17.6%	$\pm$	39.3%	31	9.7%	$\pm$	30.1%	2.5869	**	0.7276	n.s.	1.528	n.s.
	<i>pacemaker rhythm</i>	26	7.7%	$\pm$	27.2%	17	0.0%	$\pm$	0.0%	31	0.0%	$\pm$	0.0%	1.4434	n.s.	N/A	n.s.	1.443	n.s.
NT-proBNP [pg/mL]		26	2782.6	$\pm$	2290.8	17	9601.3	$\pm$	13,988.5	31	320.8	$\pm$	552.4	5.3507	***	2.7343	**	−1.992	*
troponin [pg/mL]		26	49.1	$\pm$	24.9	17	99.9	$\pm$	88.9	31	11.5	$\pm$	7.8	7.3875	***	4.0893	***	−2.299	*
eGFR <sub>MDRD</sub> [mL/min]		26	64.8	$\pm$	18.9	17	58.9	$\pm$	29.8	31	75.8	$\pm$	19.3	−2.1583	*	−2.1125	*	0.735	n.s.
septum [mm]		26	16.7	$\pm$	3.7	17	13.5	$\pm$	2.6	31	10.0	$\pm$	1.4	8.6865	***	5.0339	***	3.310	***
posterior wall [mm]		26	13.9	$\pm$	2.6	17	11.8	$\pm$	2.1	31	9.2	$\pm$	1.5	8.2203	***	4.4663	***	2.956	**
LVEF [%]		26	54.3	$\pm$	12.4	17	62.1	$\pm$	11.4	31	63.5	$\pm$	5.5	−3.5077	***	−0.4557	n.s.	−2.139	*
cardiac output [L/min]		23	4.3	$\pm$	1.5	13	6.2	$\pm$	2.7	29	5.4	$\pm$	1.2	−2.9021	***	1.0297	n.s.	−2.338	**
stroke volume [mL]		23	66.1	$\pm$	21.5	15	78.6	$\pm$	38.0	30	82.8	$\pm$	22.4	−2.7577	**	−0.3982	n.s.	−1.158	n.s.
GLPS [%]		24	−11.3	$\pm$	3.3	16	−13.4	$\pm$	4.1	30	−18.3	$\pm$	2.3	8.7357	***	4.5080	***	1.641	n.s.
apical sparing		26	100.0%	$\pm$	100.0%	17	88.2%	$\pm$	66.8%	31	45.2%	$\pm$	49.4%	2.5475	*	2.3320	n.s.	0.463	n.s.
E/A		13	1.9	$\pm$	1.4	13	2.2	$\pm$	1.0	27	1.0	$\pm$	0.3	2.2190	*	4.0794	***	−0.677	n.s.
E/E'		22	15.5	$\pm$	6.5	16	15.9	$\pm$	7.5	30	8.6	$\pm$	2.1	4.8143	***	3.8022	***	−0.156	n.s.

Table 1. Cont.

	ATTR-CA				AL-CA				Control				ATTR-CA vs. Control		AL-CA vs. Control		ATTR-CA vs. AL-CA	
n patients	26				17				31									
n observations	60				52				65									
tr-v <sub>max</sub> [m/s]	18	3.0	±	0.4	15	2.8	±	0.3	19	2.4	±	0.3	3.9130	***	3.4562	***	0.916	n.s.
% normal	8	44%			5	33%			17	89%								
% pathologic (>2.8)	10	56%			10	67%			2	11%								
diastolic dysfunction	26	73.1%	±	45.2%	17	76.5%	±	43.7%	31	12.9%	±	34.1%	5.5832	***	5.1917	***	−0.245	n.s.
acute heart failure according to ESC criteria	26	69.2%	±	47.1%	17	76.5%	±	43.7%	31	67.7%	±	47.5%	0.1184	n.s.	0.6412	n.s.	−0.515	n.s.
walking distance in 6 min walking test [m]	23	367.3	±	84.9	14	374.3	±	112.7	23	402.6	±	111.1	−1.2095	n.s.	−0.7453	n.s.	−0.199	
total bilirubin [mg/dL]	26	0.8	±	0.3	17	0.6	±	0.3	31	0.5	±	0.2	5.3905	***	1.8334	p < 0.1	1.906	p < 0.1
AP [U/L]	26	85.8	±	41.0	17	74.8	±	22.7	31	69.9	±	17.3	1.8448	p < 0.1	0.7626	n.s.	1.136	n.s.
GGT [U/L]	26	94.8	±	92.4	17	47.6	±	44.3	31	30.6	±	14.8	3.5049	***	1.5370	n.s.	2.238	*
AST [U/L]	26	34.9	±	11.7	17	29.8	±	15.2	31	25.0	±	7.8	3.6853	***	1.2144	n.s.	1.179	n.s.
ALT [U/L]	26	30.3	±	13.8	17	38.4	±	57.7	31	26.4	±	13.8	1.0577	n.s.	0.8492	n.s.	−0.575	n.s.
GLDH [U/L]	25	4.8	±	3.5	17	5.1	±	6.1	31	4.1	±	7.1	0.4327	n.s.	0.4931	n.s.	−0.204	n.s.
cholinesterase [U/L]	25	6944.7	±	1615.3	17	6287.8	±	2098.8	31	8352.9	±	1850.7	−3.0381	**	−3.3968	***	1.090	n.s.
serum albumin [g/dL]	26	4.5	±	0.2	17	3.9	±	0.7	31	4.3	±	0.8	1.2566	n.s.	−1.6510	p < 0.1	3.209	**
liver vein dilatation (%)	26	11.5%			15	6.6%			30	0.0%			5.0990	*	0.9904	n.s.	0.696	n.s.
FIB−4	26	2.77	±	0.96	17	2.34	±	1.84	31	1.37	±	0.60	6.4743	***	2.1131	**	0.896	n.s.
PDR <sub>peak</sub> [%]	22	25.9	±	7.1	13	24.5	±	5.6	27	31.3	±	15.2	−1.6334	n.s.	−2.0640	*	0.677	n.s.
stiffness [kPa]	20	7.9	±	4.5	11	5.0	±	2.0	24	5.5	±	3.3	1.9779	*	−0.6534	n.s.	2.533	*
IQR med [%]	20	24.6	±	14.0	10	16.3	±	3.8	21	22.4	±	8.9	0.5752	n.s.	−2.6804	**	2.453	*

Baseline characterisation of the analysed AmyKoS subgroups with special focus on cardiac and hepatic parameters. Differences between subgroups were analysed by z-test. \* p < 0.05, \*\* p < 0.01, \*\*\* p < 0.001; n.s. = not significant; # Gillmore stage for ATTR-CA; modified Mayo stage for AL-CA.

### 3.2. Characterisation of Hepatic Affection in CA

Mean values of AP were normal. But, in comparison to control patients, AP was elevated in ATTR-CA ( $p < 0.1$ ). AP elevation met in 7% of cases of ATTR-CA formally the definition of hepatic involvement according to Gertz et al., 2005 [11]. Mean GGT levels were elevated in both ATTR-CA and AL-CA, but reached significance only in ATTR-CA compared to the control group and AL-CA. Transaminases and GLDH were normal in all groups. Static liver synthetic function expressed by cholinesterase was reduced in both AL-CA and ATTR-CA compared to the controls, in AL-CA slightly more than in ATTR-CA. In analogy,  $PDR_{peak}$  was reduced in both forms of CA, but reached statistical significance only in AL-CA.

Moreover, AL-CA patients showed predominantly a similar stiffness compared to the control group, whereas in ATTR-CA the mean stiffness was increased to  $7.9 \pm 4.5$  kPa, which is formally in the range of F1/F2 fibrosis.

Using young healthy adults as the reference group, we found significantly lower  $PDR_{peak}$  levels in CA. The decrease was more pronounced in AL-CA than in ATTR-CA (Table S3). Analogously, the  $PDR_{peak}$  reduction was also significant, albeit less pronounced, in comparison with a healthy elderly collective. A regression regarding age in the presented CA collective showed congruent results. The extent of the  $PDR_{peak}$  reduction was comparable to findings in patients with chronic hepatitis C and those with histologically significant inflammation or fibrosis (Supplement Table S3). Moreover, the  $PDR_{peak}$  levels of patients with alcohol-induced cirrhosis Child–Pugh A or primary biliary cholangitis with LSS III were similar.

### 3.3. Effect of Cardiac Congestion on Microsomal Liver Function Expressed by $PDR_{peak}$

To get an impression of the effect of cardiac congestion on  $PDR_{peak}$ , a multivariate regression analysis referring to the panel data set was performed (Table 2): We found a significantly lower level of  $PDR_{peak}$  in AL-CA, but not in ATTR-CA. NT-proBNP was significantly negatively correlated with  $PDR_{peak}$  overall. In the subtype-specific analysis, the effect of NT-proBNP on  $PDR_{peak}$  was comparable to the overall effect for ATTR-CA, but in AL-CA, it was negligible. In contrast, liver vein dilatation was associated with a significant decrease in  $PDR_{peak}$  in the entire cohort, which was more pronounced and significant in ATTR-CA. This effect could not be calculated in the AL-CA subgroup due to multicollinearity, which indicates that the effect is comparable to the baseline effect.

To test the hypothesis that the altered pharmacokinetics of  $^{13}C$ -methacetin may result from changes in hepatic blood flow due to impaired cardiac function in AL-CA, according to the PK model published by Lane-Parashos et al. in 1986 [32],  $tr-v_{max}$  and right atrial volume were chosen as indirect surrogate parameters. A multivariate panel regression analysis showed that  $tr-v_{max}$  and right atrial volume were both inversely and significantly correlated with  $PDR_{peak}$ .

**Table 2.** Effects of congestion on  $PDR_{peak}$  and FIB-4.

NT-proBNP as congestion surrogate		$PDR_{peak}$ HR (95% CI)	FIB-4 HR (95% CI)
n observations		148	177
constant		29.805 *** [25.646; 33.964]	1.451 *** [1.218; 1.684]
cardiac manifestation	ATTR-CA	−0.737 [−6.593; 5.118]	1.352 *** [0.520; 2.185]
	AL-CA	−5.849 ** [−10.460; −1.238]	0.600 * [−0.053; 1.253]
	overall	−1.726 ** [−3.445; −0.006]	0.036 [−0.034; 0.107]
NT-proBNP #	ATTR-CA	0.787 [−1.216; 2.789]	−0.039 [−0.189; 0.112]
	AL-CA	1.652 * [−0.070; 3.374]	−0.020 [−0.096; 0.057]

**Table 2.** Cont.

liver vein dilation as congestion surrogate			
n observations		143	172
constant		28.921 *** [25.182; 32.660]	1.478 *** [1.255; 1.700]
cardiac manifestation	ATTR-CA	−1.429 [−6.311; 3.453]	1.326 *** [0.774; 1.878]
	AL-CA	−5.130 ** [−9.533; −0.726]	0.700 ** [0.034; 1.367]
dilated liver veins	overall	−2.240 * [−4.738; 0.258]	−0.168 [−1.242; 0.907]
	ATTR-CA	−6.021 ** [−11.390; −0.653]	0.304 [−0.893; 1.501]
	AL-CA	##	##

The 95% confidence intervals (95% CI) in brackets; \*  $p < 0.1$ , \*\*  $p < 0.05$ , \*\*\*  $p < 0.01$ ; # in 1000 pg/mL; ## dropped due to multicollinearity. A multivariate regression analysis based on the panel data set was performed to evaluate the effect of cardiac congestion on  $PDR_{peak}$  and FIB-4. NT-proBNP and dilated liver veins were chosen as surrogates for congestion:  $PDR_{peak}$  was significantly reduced in AL-CA (column 1:  $b_{NT-proBNP} = -5.849$ ,  $p < 0.05$ ;  $b_{liver\ vein\ dilation} = -5.130$ ,  $p < 0.05$ ), but not in ATTR-CA (column 1:  $b_{NT-proBNP} = -0.737$ ,  $p > 0.1$ ;  $b_{liver\ vein\ dilation} = -1.429$ ,  $p > 0.1$ ). NT-proBNP was significantly negatively correlated with  $PDR_{peak}$  overall (column 1:  $b_{overall} = -1.726$ ,  $p < 0.05$ ). The effect of NT-proBNP on  $PDR_{peak}$  was comparable to the overall effect for ATTR-CA (column 1:  $b_{ATTR-CA} = 0.787$ ,  $p > 0.1$ ), but in AL-CA it was negligible because both the overall (column 1:  $b_{overall} = -1.726$ ,  $p < 0.05$ ) and the group-specific effect (column 1:  $b_{AL-CA} = 1.652$ ,  $p < 0.1$ ) were significant and their sum was close to zero. Liver vein dilatation was associated with a significant decrease in  $PDR_{peak}$  overall (column 1:  $b_{overall} = -2.240$ ,  $p < 0.1$ ), which was more pronounced and significant in ATTR-CA in the subtype-specific analysis (column 1:  $b_{ATTR-CA} = -6.021$ ,  $p < 0.05$ ). This effect could not be calculated in the AL-CA subgroup due to multicollinearity indicating that the effect is comparable to the baseline effect. Both AL-CA (column 2:  $b_{NT-proBNP} = 0.600$ ,  $p < 0.1$ ;  $b_{liver\ vein\ dilation} = -0.700$ ,  $p < 0.05$ ) and ATTR-CA (column 2:  $b_{NT-proBNP} = 1.352$ ,  $p < 0.01$ ;  $b_{liver\ vein\ dilation} = 1.326$ ,  $p < 0.01$ ) showed a significant baseline effect on FIB-4, but there was no significant effect on FIB-4 by NT-proBNP and liver vein dilatation.

### 3.4. Chronic Liver Damage and Fibrosis in Cardiac Amyloidosis

To assess the role of possible fibrotic processes in CA, we calculated the well-established fibrosis score FIB-4 according to the generally applicable formula (see above in Section 2). At baseline evaluation, 17.6% of AL-CA, 30.7% of ATTR-CA and 0% of controls showed FIB-4 scores  $> 3.2$ , a value compatible with a high risk of advanced liver cirrhosis. The increase in FIB-4 was correlated with  $PDR_{peak}$ , but an apparent threshold for  $PDR_{peak}$  with an altered increase in FIB-4 could not be detected. The effect of NT-proBNP and liver vein congestion on FIB-4 was analysed by multivariate panel regression in analogy to the effect on  $PDR_{peak}$  because FIB-4 includes AST and ALT as congestion-sensitive parameters (Table 2). Both AL-CA and ATTR-CA showed a significant baseline effect on FIB-4, but there was no significant effect on FIB-4 by NT-proBNP and liver vein dilatation.

Additionally, the congestion-dependent component of FIB-4 was estimated by linear regression to be between 0.2% in ATTR-CA and 3.7% in AL-CA (overall, 3.0%).

### 3.5. Modelling Liver Affection in Cardiac Amyloidosis

Against the background of the previous results and considerations, we chose liver stiffness as a summatory surrogate for liver affection going beyond fibrosis and adapted the theoretical model proposed by Müller et al., 2010 [30] to the special situation in cardiac amyloidosis (in the absence of hepatic involvement), as shown in Figure 1.

As subtype-spanning main influencing factors the following parameters were defined: severity of cardiac involvement with resulting impairment of cardiac function, cardiac congestion, inflammation and chronic liver cell damage including fibrosis. Clinical, laboratory and instrumental surrogate parameters were assigned to the defined main influencing factors, and the surrogates for the final regression model were selected based on the literature, their clinical value and availability in daily practice, as well as the results of a Spearman correlation analysis (Figure 1; Table S4). High-sensitive troponin and C-reactive protein showed no predictive power for liver stiffness, so these parameters were also subsequently dropped.

Based on this, the estimation of the regression model was performed and subgroup-specific coefficients were calculated as shown in Table 3 and visualised in Figure 2. To test the generalisability of the approach and the stability of the results, we estimated the

regression model for the subgroup of patients with localised amyloidosis who can be considered as healthy controls (model 1) and for the entire control group, including patients with non-amyloidotic cardiac disorders (model 2).

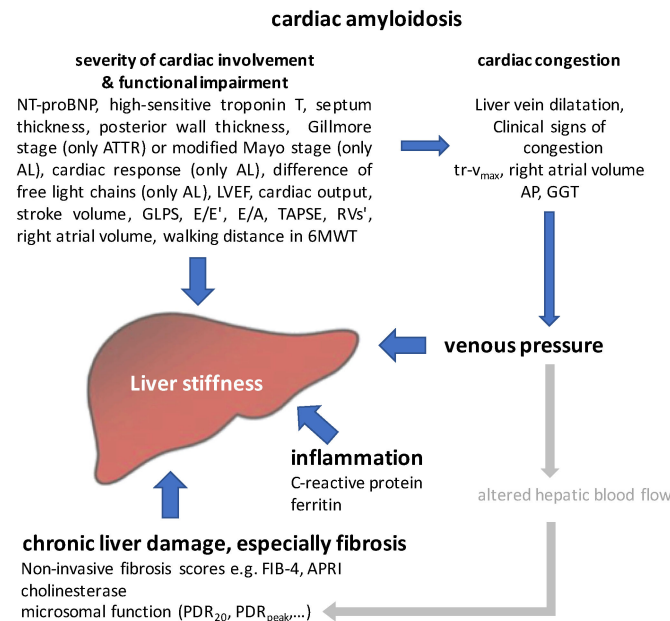


**Figure 1.** Theoretical model of the cardio-hepatic crosstalk in cardiac amyloidosis (based on the model of Müller et al., 2010 [30] and specifically adapted to cardiac amyloidosis). VCTE is usually applied in patients with a high a priori probability of liver fibrosis due to chronic liver disease and, therefore, stiffness primarily reflects in these patients the grade of liver fibrosis. In contrast, in cardiac amyloidosis, the proposed application of VCTE occurs early in the development of possible fibrosis (so-called cirrhosis cardiaque) and increased stiffness may also result from chronic cardiac congestion. Subtype-spanning main influencing factors for liver stiffness in cardiac amyloidosis are supposed to be the severity of cardiac involvement with resulting impairment of cardiac function, cardiac congestion, inflammation and chronic liver cell damage including fibrosis. Potential clinical, laboratory and instrumental surrogate parameters were assigned based on the literature, their clinical value and availability.

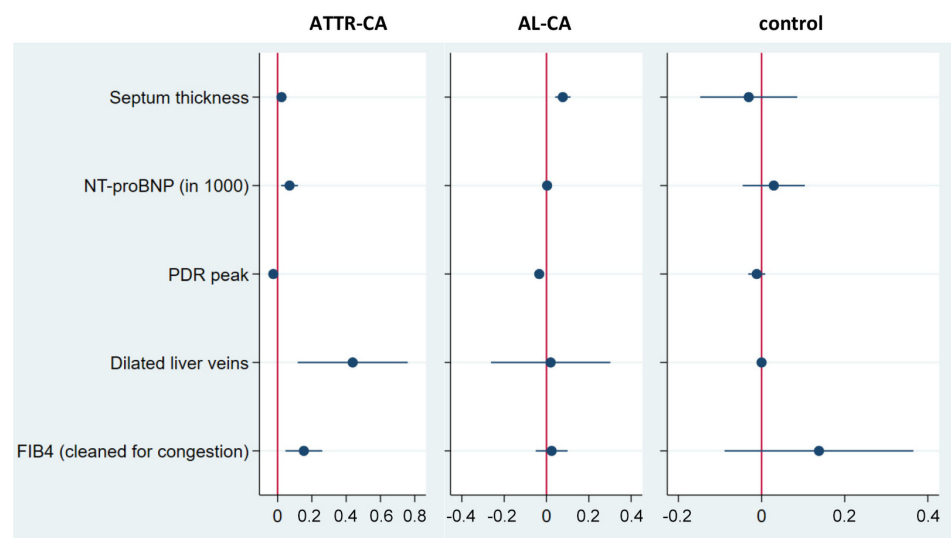


**Figure 2.** Visualisation of the coefficients of the post-cluster LASSO referring to model 2 (blue dot = regression coefficient; blue lines = 95% confidence intervals).

**Table 3.** Results of post-cluster LASSO.

		Model 1	Model 2
n observations		76	101
n patients		35	52
Core Variables		Log Liver Stiffness	Log Liver Stiffness
septum thickness	control	−0.136 ** [−0.255; −0.016]	−0.032 [−0.149; 0.085]
	ATTR-CA	0.021 ** [0.002; 0.040]	0.023 ** [0.002; 0.044]
	AL-CA	0.055 *** [0.016; 0.094]	0.077 *** [0.041; 0.113]
NT-proBNP	control	1.722 ** [0.165; 3.279]	0.036 [−0.032; 0.105]
	ATTR-CA	0.069 *** [0.028; 0.111]	0.070 *** [0.021; 0.118]
	AL-CA	0.002 [−0.002; 0.007]	0.003 [−0.001; 0.008]
PDR <sub>peak</sub>	control	−0.003 [−0.018; 0.012]	−0.014 [−0.033; 0.004]
	ATTR-CA	−0.026 *** [−0.041; −0.011]	−0.025 *** [−0.040; −0.010]
	AL-CA	−0.031 *** [−0.048; −0.015]	−0.034 *** [−0.051; −0.017]
dilated liver veins	control	#	#
	ATTR-CA	0.376 ** [0.064; 0.688]	0.438 *** [0.117; 0.759]
	AL-CA	0.066 [−0.229; 0.362]	0.020 [−0.262; 0.302]
FIB-4 <sub>clean</sub>	control	0.132 [−0.230; 0.494]	0.179 [−0.205; 0.564]
	ATTR-CA	0.144 *** [0.043; 0.245]	0.153 *** [0.046; 0.260]
	AL-CA	0.011 [−0.064; 0.087]	0.024 [−0.051; 0.099]
LASSO-selected controls		AL-CA, ATTR-CA, AP, TAPSE	AL-CA, ATTR-CA, AP
constant		3.215 *** [1.544; 4.885]	2.359 *** [0.994; 3.725]

The 95% confidence intervals are in brackets; \*  $p < 0.1$ , \*\*  $p < 0.05$ , \*\*\*  $p < 0.01$ . Each of the two columns represents a multivariate regression of the log normalized liver stiffness on the core variables and the high-dimensional controls selected by post-cluster LASSO. The core variables of interest were septum thickness, NT-proBNP, PDR<sub>peak</sub> and dilation of liver veins within both models pre-selected based on Figure 1. Coefficients for liver vein dilation (#) were not identified, as there was no patient with dilated hepatic veins among the control group. The control group used in model 1 included only the subset of control patients with localised amyloidosis without cardiac impairment, whereas model 2 referred to the entire control group with a high percentage of patients suffering from other cardiac disorders.

We were able to prove that septum thickness, NT-proBNP and PDR<sub>peak</sub> are predictors of liver stiffness in ATTR-CA and AL-CA in both models. Dilated liver veins and FIB-4<sub>clean</sub> predicted liver stiffness only for ATTR-CA. The inclusion of tr-v<sub>max</sub> in the models resulted in computational instability (Table S5). However, tr-v<sub>max</sub> seemed to be a predictor for liver stiffness, but only in AL-CA.

### 3.6. Predictive Value of the Main Influencing Factors Regarding All-Cause Mortality

The median follow-up of the observed patient population was 666 days and, in total, 12 patients died. The Kaplan–Meier survival curves for AL-CA, ATTR-CA and the control group are shown in Figure 3.

The predictive value of liver stiffness and the chosen main influencing factors of our model regarding all-cause mortality were analysed by Cox proportional hazard survival regression. Additionally, in cardiac AL and ATTR amyloidosis, the well-established prognostic marker high-sensitive troponin was added.

Liver stiffness, high-sensitive troponin, NT-proBNP and PDR<sub>peak</sub> were significant predictors of all-cause mortality (Table 4; Figure 4). Septum thickness, dilated liver veins and FIB-4<sub>clean</sub> were not able to predict prognosis.

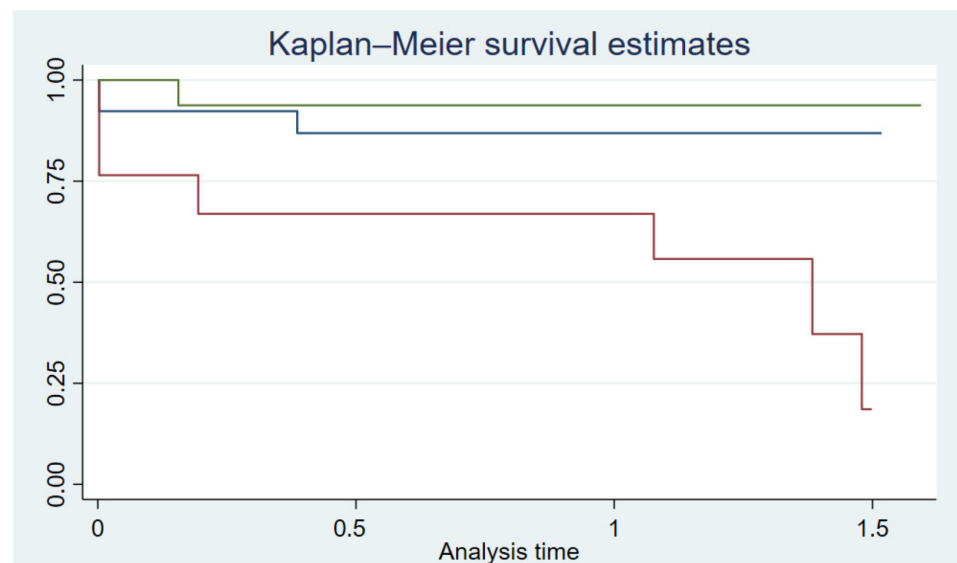


**Figure 3.** The Kaplan–Meier curves illustrate the overall survival among the three groups (ATTR-CA blue line; AL-CA red line; controls green line). The X-axis reflects the observation time in years; the Y-axis indicates the proportion of patients still alive.

**Table 4.** COX analysis.

COX Analysis	1 HR [95% CI]	2 HR [95% CI]
liver stiffness	1.744 ** [1.136; 2.678]	
NT-proBNP (in 1000)	1.025 * [0.997; 1.054]	
hs-TNT	1.120 ** [1.027; 1.222]	
PDR <sub>peak</sub>	1.305 *** [1.079; 1.579]	
dilated liver veins		14.101 [0.244; 813.970]
septum thickness		1.062 [0.876; 1.288]
FIB-4 <sub>clean</sub>		2.798 [0.365; 21.425]
n observations	105	105
Pseudo R <sup>2</sup>	0.642	0.272

Exponentiated coefficients; 95% confidence intervals in brackets. \*  $p < 0.1$ , \*\*  $p < 0.05$ , \*\*\*  $p < 0.01$ . Cox proportional hazard regression (Cox survival regression) was used to evaluate the ability of the parameters used in the initial LASSO regression model (stiffness, septum thickness, NT-proBNP, liver vein dilatation, PDR<sub>peak</sub>) to predict mortality risk. High-sensitive troponin, NT-proBNP, PDR<sub>peak</sub> and liver stiffness were able to predict prognosis (column 1) in contrast to septum thickness, dilated liver veins and FIB-4<sub>clean</sub> (column 2).

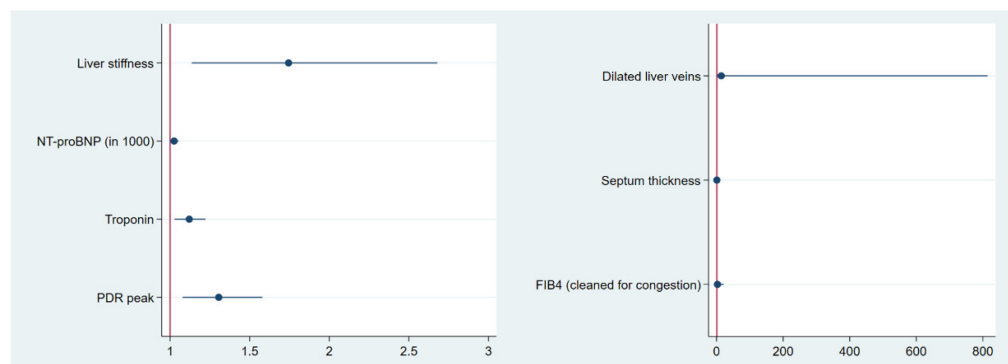


**Figure 4.** Forest plot for the visualisation of the association between influencing factors and all-cause mortality (blue dot = regression coefficient; blue lines = 95% confidence intervals).

#### 4. Discussion

This study aimed to (1) non-invasively characterise and model secondary liver affection in CA and (2) assess the diagnostic and prognostic value of dynamic liver function tests and VTCE.

In the light of this, the most relevant findings are the following:

- A significant proportion of ATTR-CA patients (7%) in our sample present with AP elevation and therefore formally fulfil the criteria for liver involvement according to Gertz et al., 2005 [11].
- Secondary liver affection in ATTR-CA results in decreased microsomal liver function related to hepatic congestion.
- Reduced  $PDR_{peak}$  in AL-CA may result from altered pharmacokinetics due to changed hepatic blood flow.
- Liver stiffness may act as a summatory surrogate for liver affection going beyond fibrosis and also reflects impaired cardiac function in CA, hypervolemia and congestion. Based on this, we were able to model the interaction between liver and heart in ATTR-CA and AL-CA: septum thickness, NT-proBNP and  $PDR_{peak}$  have been identified as predictors of liver stiffness for both entities. The dilatation of liver veins and  $FIB-4_{clean}$  are significant predictors only in ATTR-CA.
- Liver stiffness, high-sensitive troponin, NT-proBNP and  $PDR_{peak}$  are predictors of all-cause mortality, suggesting them as promising factors for risk stratification in cardiac amyloidosis.

So far, little is known about the congestion-related effects of cardiac dysfunction in CA on other organs, especially the liver, particularly the functional (biochemical) and physical (stiffness, matrix deposition) consequences. Moreover, their prognostic relevance is still unclear.

The fact that 7% of the ATTR amyloidosis patients in our sample present with elevated AP levels according to the definition by Gertz et al., 2005 [11] implies that AP is not very specific and may not specifically differentiate between primary and secondary liver affection in AL-CA. AP has to be applied cautiously and examined on a case-by-case basis. More robust and generally applicable parameters for the distinction of primary and secondary liver affection are needed, which can also be supported by the finding that AP seems to identify only part of patients with liver involvement, according to Brunger et al. [33]. Whether or not VCTE and/or compartment-specific  $^{13}C$ -breathing tests such as  $^{13}C$ -methacetin and  $^{13}C$ -methionin breath tests might be helpful in this context has to be investigated in further studies.

Normal levels of transaminases and GLDH do not indicate acute ongoing hepatocyte damage in cardiac amyloidosis. Nevertheless, we were able to show that secondary liver affection is significantly underestimated in the context of CA.

In ATTR-CA, a considerably lower liver synthesis capacity as measured by cholinesterase ( $p < 0.01$ ) and an impaired (albeit not significant) microsomal function as proxied by  $^{13}C$ -methacetin breath testing ( $PDR_{peak}$ ) can be observed compared to the control patients. The fact that chronic cardiac impairment negatively impacts hepatic function is not new. Therefore, Malek et al. could demonstrate a significantly impaired metabolic liver function in a small cohort of patients with advanced chronic heart failure [34]. Functional liver mass did not correlate with LVEF, but left atrial diameter did [34]. According to another pilot study published by Hendrichová et al., 2010, the correlation of NT-proBNP with the degree of metabolic liver function impairment did not reach significance in patients with decompensated heart failure [35].

However, the extent of hepatic impairment comparable to an alcohol-induced cirrhosis Child–Pugh A or primary biliary cholangitis with LSS III seems surprising at first glance. However, given that the patients typically develop a renal deterioration in the sense of a cardiorenal syndrome type II in the course of their disease, which is used in the well-established algorithm for risk stratification published by Gillmore et al. [6,36], the observation appears plausible.

In contrast, lower  $PDR_{peak}$  levels in AL-CA most likely result in altered blood flow with consecutive changes in pharmacokinetics. This assumption is based on a multivariate panel regression showing that  $tr-v_{max}$  and right atrial volume were both inversely and significantly correlated with  $PDR_{peak}$ . Of course, a direct and invasive measurement of hepatic blood flow by right heart catheter would be desirable to prove this hypothesis, but was not justifiable for patient safety reasons and a known high risk of bleeding in amyloidosis. At the same time, altered blood flow with resulting changes in pharmacokinetics is already known from other confounders such as inflammation, hepatocellular proliferation and hypoxia. Moreover, the high dynamics of cardiac dysfunction in AL-CA have been extensively investigated. The direct cardiotoxicity of circulating free light chains results in an immediate decrease in cardiac function after the infusion of free light chains in animal models such as zebrafish and mouse hearts [7].

In analogy to other chronic liver diseases and given the clinical picture of cirrhotic cardiaque, it can be assumed that fibrotic processes may also play a role in this context. Because of the high risk of bleeding in systemic amyloidosis and comparatively low stiffness values that do not justify liver biopsies at this stage of knowledge, a primarily non-invasive approach was chosen for patient safety. As the available non-invasive fibrosis markers are not validated as single direct markers in this context and the established fibrosis scores include at least one congestion-sensitive parameter, e.g., AST, ALT and GGT, we used FIB-4 corrected for the effect of mere congestion (e.g., on the AST to ALT ratio) as a surrogate score for hepatic fibrosis and indicator of increased matrix deposition during CA.

While the clinical assessment of signs of hypervolemia such as oedema, jugular venous congestion, etc., or diuretic use only represents a current snapshot and may be absent in amyloidosis as restrictive cardiomyopathy, liver stiffness might represent a combined surrogate parameter. It might reflect currently detectable hepatic congestion in the context of acute cardiac decompensation, but also chronic effects such as fibrotic processes as “long-term memory” for recurrent damage and repair during acute and chronic cardiac congestion frequently observed in the long-term course of ATTR-CA. These associations were successfully modelled across subtypes in AL-CA and ATTR-CA using state-of-the-art statistical methods. According to the model, hepatic venous congestion and fibrotic processes play a significant role in secondary liver affection in ATTR-CA. Increased liver stiffness may indicate advanced disease stages. Against this background, it is not surprising that liver stiffness serves as an additional predictor of mortality beyond cardiac biomarkers. The negative impact of hypervolemia and recurrent cardiac decompensations is well known for heart failure in general. This also fits with the findings of Gillmore et al. that a reduced eGFR in the sense of cardiorenal syndrome type 2 is prognostically relevant in ATTR-CA and the staging system can be applied serially [6,36].

Considering the direct cardiotoxicity of the free light chains in AL-CA with direct NT-proBNP increase [37], it is conceivable that hepatic venous congestion and fibrosis processes take a background role given the predominance of NT-proBNP in AL-CA.

In light of the presented results and considerations, liver stiffness does not appear to be a useful tool for improving early diagnosis because liver fibrosis due to primary liver disorders is much more frequently found and hepatic congestion is common in heart failure. However, liver stiffness is of prognostic relevance and may indicate advanced stages. While in cardiac AL amyloidosis, high-risk groups with short survival such as Mayo stage IIIB with median survival of < 6 months can be identified based on cardiac biomarkers, the temporal resolution of the staging systems published to date for ATTR-CA is 20–24 months for the high-risk group [5,6,38]. A further resolution of the mortality risk would be of daily relevance. Therefore, liver stiffness might be useful in identifying high-risk patients requiring intensive monitoring and without the benefit of disease-modifying treatments. It would allow for the more efficient use of resources by implementing it in the clinical pathway after diagnosis against the backdrop of improved awareness and increasing numbers of newly diagnosed patients [39,40].

Liver vein dilation was chosen as the primary surrogate for congestion in our analysis, as it was a clearly defined measure with low investigator dependency on the one hand. On the other hand, a correlation analysis regarding liver stiffness showed that there were significant correlations between liver stiffness and echo-based assessed congestion markers such as  $tr-v_{max}$ , liver vein dilation and right atrial volume, whereas the number of diuretics, diuretic equivalence dose, neck vein dilation, oedema and the combined scores of clinical congestion signs failed to reach significance. Of course, the effect of the small number of subjects can be discussed in this context, especially as the assessment of clinical parameters may be more variable than the standardised assessment of defined echocardiographic parameters by experienced echocardiographers. However, clinical experience shows that amyloidosis patients, as typical examples of restrictive cardiomyopathy, are often hypervolemic even in the absence of classic signs of heart failure such as oedema. It remains to be evaluated which is the best parameter for detecting hypervolemia in cardiac amyloidosis and whether there may also be subtype-specific differences.

The limitations of our study are the non-availability of a liver biopsy for histological correlation, which would have been desirable as the gold standard for the detection and staging of fibrosis and a possible inflammatory component. Because of this particular bleeding risk, there is a complete lack of previous histological data up to now and the congestion-adjusted version of the FIB-4 appears to be an acceptable surrogate parameter with careful risk–benefit consideration. As the analyses refer to the data set of a registry study, a dedicated control group for heart failure is not available. We addressed this issue by selecting a mixed control group consisting of patients with excluded cardiac amyloidosis, including patients with signs of heart failure (approximately 40% of NYHA stage II–III patients in the control group). The post-cluster LASSO was additionally performed with the subgroup of localised amyloidosis, which is considered to be cardiac-healthy patients, to get an idea of possible differences.

Due to the small number of cases, the results have to be considered exploratory and require further confirmation and validation. The small case number was addressed by using a panel data set and a cross-subtype analysis with subsequent consideration of the respective group due to the different pathomechanisms. At the same time, however, the cross-subtype approach allows for better generalisability.

Future investigations regarding the validation of the results in an independent cohort, as well as the comparison with other cardiac diseases, but also the development of stratification algorithms with liver stiffness in combination with other parameters, appear promising. A precise characterisation of the metabolic limitations in the various subtypes of amyloidosis may allow for the identification of a specific pattern in the long term, which can be used in dedicated centres for the non-invasive diagnosis of hepatic amyloidosis.

## 5. Conclusions

Clinical findings and in daily practice established liver function tests such as AP fail to differentiate between primary and secondary liver affection in CA. Liver stiffness might be a promising clinical tool for combined imaging of liver fibrosis, impaired cardiac function, hypervolemia and congestion in a time-sparing and easy-to-use manner. Reduced microsomal liver function in ATTR-CA seems to be related to hepatic congestion, whereas lower values in AL-CA may be explained by changed hepatic blood flow. Liver stiffness is a predictor of all-cause mortality and might be a promising parameter for risk stratification in cardiac amyloidosis, but further investigation and confirmation are required.

**Supplementary Materials:** The following supporting information can be downloaded at: <https://www.mdpi.com/article/10.3390/jcm13051440/s1>, Table S1: Overview of diagnostic investigations to assess liver affection in cardiac amyloidosis; Table S2: Additional information on clinical signs of congestion/hypervolemia and medication; Table S3: Comparison of PDRpeak among different patient collectives; Table S4: Surrogate parameters for the main influencing factors and the rationale of their choice; Table S5: Results of post-cluster LASSO with addition of  $tr-v_{max}$  as surrogate of acutal volume status.

**Author Contributions:** S.M.I.-S.: development of design of the AmyKoS study; writing of study protocol and preparation of ethic application; development of the hypothesis of the manuscript; data analysis, interpretation of results and writing of the manuscript; O.G.: analysis and interpretation of breath tests and VTCE results, provision of reference cohort data and review of the manuscript; F.G.: data acquisition and review of the manuscript; F.S.: review of the manuscript; I.S.: data analysis, interpretation of echocardiography and review of the manuscript; A.P.: review of the manuscript; C.M.: review of the manuscript; S.F.: review of the manuscript; H.E.: review of the manuscript; S.K.: review of the manuscript; C.S.: review of the manuscript; B.M.: provision of reference cohort data and review of the manuscript; T.S.: data analysis, interpretation of statistics and writing of the manuscript; S.S.: writing and review of study protocol and review of the manuscript; A.G.: data interpretation and writing of the manuscript. All authors have read and agreed to the published version of the manuscript.

**Funding:** Sandra Ihne-Schubert was a fellow of the local Clinician Scientist program of the Interdisciplinary Center of Clinical Research—IZKF, Würzburg (2018–2021, Z-2\_CSP-08).

**Institutional Review Board Statement:** This study complies with the Declaration of Helsinki and received positive votes from the Medical Ethics Committee at the Julius-Maximilians-University of Würzburg (48/18) (approval date 13 July 2018).

**Informed Consent Statement:** All participants provided written informed consent.

**Data Availability Statement:** Data cannot be shared in public due to privacy regulations and patient consent.

**Acknowledgments:** The authors thank the participating patients.

**Conflicts of Interest:** Sandra Ihne-Schubert: received financial reimbursement for consulting, advisory board activities, speaker honoraries and/or travel support to attend scientific meetings by Akcea Therapeutics, Alnylam, Pfizer, Janssen-Cilag and Takeda, and further research funding from Pfizer and Akcea Therapeutics. An internship was supported by ONLUS. She was a fellow of the local Clinician Scientist program of the IZKF Würzburg. Oliver Goetze: no conflicts of interest. Felix Gerstendörfer: no conflicts of interest. Florian Sahiti: no conflicts of interest. Ina Schade: no conflicts of interest. Aikaterini Papagianni: received research funding grant from Pfizer, consulting fees from Pfizer, Alnylam, Akcea and Swedish Orphan Biovitrum GmbH-Sobi, financial support for attending meetings and/or travel from Alnylam, Akcea and Pfizer. Aikaterini Papagianni is also PI in ION-682884-CS3 study. She is supported by the IZKF Würzburg (habilitation scholarship). Caroline Morbach: research cooperation with the University of Würzburg and Tomtec Imaging Systems, funded by a research grant from the Bavarian Ministry of Economic Affairs, Regional Development and Energy, Germany; she is supported by the German Research Foundation (DFG) within the Comprehensive Research Center 1525 ‘Cardio-immune Interfaces’ (453989101, project C5) and received financial support from the Interdisciplinary Center for Clinical Research—IZKF, Würzburg (advanced clinician-scientist program; AdvCSP 3). She further received advisory and speakers honoraria as well as travel grants from Tomtec, Alnylam, AKCEA, Pfizer, Boehringer Ingelheim, SOBI, AstraZeneca, NovoNordisk, Alexion, Janssen and EBR Systems, and acted as principal investigator in trials sponsored by Alnylam, Bayer, NovoNordisk and AstraZeneca. Stefan Frantz: received consultancy and lecture fees as well as travel expenses from AMGEN Europe, AstraZeneca, Bayer Vital, Boehringer Ingelheim, Bristol-Meyers Squibb GmbH, Daiichi Sankyo, MSD, Novartis, Pfizer, Sanofi, Servier and Vifor. Hermann Einsele: no conflicts of interest. Stefan Knop: no conflicts of interest. Claudia Sommer: received speaker honoraria from Alnylam. Beat Müllhaupt: no conflicts of interest. Torben Schubert: no conflicts of interest. Stefan Störk: received research support from the German Federal Ministry of Education and Research (BMBF). He has received consultancy and lecture fees from Akcea, AstraZeneca, Bayer, Boehringer Ingelheim, Novartis, Novo Nordisk and Pfizer. His department received case payments for study participation from Akcea Therapeutics, Alnylam and IONIS. Andreas Geier: served as steering committee member or advisor for AbbVie, Alexion, Bayer, BMS, Eisai, Falk, Gilead, Heel, Intercept, Ipsen, Merz, MSD, Novartis, Pfizer, Roche, Sanofi-Aventis and as speaker for AbbVie, Advanz, Alexion, BMS, Burgerstein, CSL Behring, Falk, Gilead, Intercept, Merz, MSD, Novartis, Roche. He received research support from Intercept, Falk (both NAFLD CSG) and Novartis.

## Abbreviations

AL amyloidosis	systemic light chain amyloidosis
AL-CA	cardiac light chain amyloidosis
ALF	acute liver failure
ALT	alanine aminotransferase (=GPT)
AP	alkaline phosphatase
APRI	AST to platelet ratio index
AST	aspartate aminotransferase (=GOT)
ATTR amyloidosis	transthyretin amyloidosis
ATTR-CA	cardiac transthyretin amyloidosis
AUC	area under the curve
CA	cardiac amyloidosis
COX survival regression	Cox proportional hazard regression
CYP1A2	cytochrome P450 1A2
ECOG Performance Status	Eastern Cooperative Oncology Group Performance Status
eGFR	estimated glomerular filtration rate
FIB-4 (score)	fibrosis-4 (score)
FIB-4 <sub>clean</sub>	fibrosis-4 (score) cleaned for its statistical component related to congestion by regressing the score on NT-proBNP and liver vein congestion
GGT	gamma-glutamyl transferase
GLDH	glutamate dehydrogenase
GLPS	global longitudinal strain
GOT	aspartate aminotransferase (AST)
GPT	alanine aminotransferase (ALT)
HCV	hepatitis C virus
HFpEF	heart failure with preserved ejection fraction
IQR	interquartile range
IQR med	IQR/median
kPa	kilopascal
LASSO	least absolute shrinkage and selection operator regression
LVEF	left ventricular ejection fraction
LSS	Ludwig's staging system
MAPK pathway	mitogen-activated protein kinase pathway
MBT	<sup>13</sup> C-methacetin breath test
ML	machine learn
NT-proBNP	N-terminal pro-brain natriuretic peptide
NYHA	New York Heart Association
PBC	primary biliary cholangitis
PDR <sub>peak</sub>	maximal percentage of dose rate
PDR <sub>20</sub>	percentage of dose rate at 20 min
PK model	pharmacokinetic model
posterior wall	left ventricular posterior wall
septum	interventricular septum
TAPSE	tricuspid annular plane systolic excursion
tr-v <sub>max</sub>	maximal tricuspid regurgitation velocity
ULN	upper limit of normal
VTCE	vibration-controlled transient elastography
6MWT	6 min walk test

## References

1. Ihne, S.; Morbach, C.; Obici, L.; Palladini, G.; Stork, S. Amyloidosis in Heart Failure. *Curr. Heart Fail. Rep.* **2019**, *16*, 285–303. [[CrossRef](#)] [[PubMed](#)]
2. Ihne, S.; Morbach, C.; Sommer, C.; Geier, A.; Knop, S.; Störk, S. Amyloidosis—The diagnosis and treatment of an underdiagnosed disease. *Dtsch. Arztebl. Int.* **2020**, *117*, 159–166. [[CrossRef](#)] [[PubMed](#)]
3. Palladini, G.; Sachchithanatham, S.; Milani, P.; Gillmore, J.; Foli, A.; Lachmann, H.; Basset, M.; Hawkins, P.; Merlini, G.; Wechalekar, A.D. A European collaborative study of cyclophosphamide, bortezomib, and dexamethasone in upfront treatment of systemic AL amyloidosis. *Blood* **2015**, *126*, 612–615. [[CrossRef](#)] [[PubMed](#)]

4. Grogan, M.; Dispenzieri, A. Natural history and therapy of AL cardiac amyloidosis. *Heart Fail. Rev.* **2015**, *20*, 155–162. [[CrossRef](#)] [[PubMed](#)]
5. Grogan, M.; Scott, C.G.; Kyle, R.A.; Zeldenrust, S.R.; Gertz, M.A.; Lin, G.; Klarich, K.W.; Miller, W.L.; Maleszewski, J.J.; Dispenzieri, A. Natural History of Wild-Type Transthyretin Cardiac Amyloidosis and Risk Stratification Using a Novel Staging System. *J. Am. Coll. Cardiol.* **2016**, *68*, 1014–1020. [[CrossRef](#)]
6. Gillmore, J.D.; Damy, T.; Fontana, M.; Hutchinson, M.; Lachmann, H.J.; Martinez-Naharro, A.; Quarta, C.C.; Rezk, T.; Whelan, C.J.; Gonzalez-Lopez, E.; et al. A new staging system for cardiac transthyretin amyloidosis. *Eur. Heart J.* **2017**, *39*, 2799–2806. [[CrossRef](#)]
7. Mishra, S.; Guan, J.; Plovie, E.; Seldin, D.C.; Connors, L.H.; Merlini, G.; Falk, R.H.; MacRae, C.A.; Liao, R. Human amyloidogenic light chain proteins result in cardiac dysfunction, cell death, and early mortality in zebrafish. *Am. J. Physiol. Heart Circ. Physiol.* **2013**, *305*, H95–H103. [[CrossRef](#)]
8. Mishra, S.; Joshi, S.; Ward, J.E.; Buys, E.P.; Mishra, D.; Mishra, D.; Morgado, I.; Fisch, S.; Lavatelli, F.; Merlini, G.; et al. Zebrafish model of amyloid light chain cardiotoxicity: Regeneration versus degeneration. *Am. J. Physiol. Heart Circ. Physiol.* **2019**, *316*, H1158–H1166. [[CrossRef](#)]
9. Shi, J.; Guan, J.; Jiang, B.; Brenner, D.A.; Del Monte, F.; Ward, J.E.; Connors, L.H.; Sawyer, D.B.; Semigran, M.J.; Macgillivray, T.E.; et al. Amyloidogenic light chains induce cardiomyocyte contractile dysfunction and apoptosis via a non-canonical p38alpha MAPK pathway. *Proc. Natl. Acad. Sci. USA* **2010**, *107*, 4188–4193. [[CrossRef](#)]
10. Milani, P.; Merlini, G.; Palladini, G. Light Chain Amyloidosis. *Mediterr. J. Hematol. Infect. Dis.* **2018**, *10*, e2018022. [[CrossRef](#)]
11. Gertz, M.A.; Comenzo, R.; Falk, R.H.; Feraud, J.P.; Hazenberg, B.P.; Hawkins, P.N.; Merlini, G.; Moreau, P.; Ronco, P.; Sanchowala, V.; et al. Definition of organ involvement and treatment response in immunoglobulin light chain amyloidosis (AL): A consensus opinion from the 10th International Symposium on Amyloid and Amyloidosis. *Am. J. Hematol.* **2005**, *79*, 319–328. [[CrossRef](#)]
12. Kaswala, D.H.; Lai, M.; Afdhal, N.H. Fibrosis Assessment in Nonalcoholic Fatty Liver Disease (NAFLD) in 2016. *Dig. Dis. Sci.* **2016**, *61*, 1356–1364. [[CrossRef](#)]
13. Chalasani, N.; Younossi, Z.; Lavine, J.E.; Charlton, M.; Cusi, K.; Rinella, M.; Harrison, S.A.; Brunt, E.M.; Sanyal, A.J. The diagnosis and management of nonalcoholic fatty liver disease: Practice guidance from the American Association for the Study of Liver Diseases. *Hepatology* **2018**, *67*, 328–357. [[CrossRef](#)]
14. National Guideline Centre (UK). *Non-Alcoholic Fatty Liver Disease: Assessment and Management*; National Institute for Health and Care Excellence (NICE): London, UK, 2016.
15. Holzhutter, H.G.; Lock, J.F.; Taheri, P.; Bulik, S.; Goede, A.; Stockmann, M. Assessment of hepatic detoxification activity: Proposal of an improved variant of the (13)c-methacetin breath test. *PLoS ONE* **2013**, *8*, e70780. [[CrossRef](#)]
16. Keller, J.; Hammer, H.F.; Afolabi, P.R.; Benninga, M.; Borrelli, O.; Dominguez-Munoz, E.; Dumitrascu, D.; Goetze, O.; Haas, S.L.; Hauser, B.; et al. European guideline on indications, performance and clinical impact of (13) C-breath tests in adult and pediatric patients: An EAGEN, ESNM, and ESPGHAN consensus, supported by EPC. *United Eur. Gastroenterol. J.* **2021**, *9*, 598–625. [[CrossRef](#)] [[PubMed](#)]
17. Ozercan, A.M.; Ozkan, H. Vibration-controlled Transient Elastography in NAFLD: Review Study. *Eur. J. Hepatogastroenterol.* **2022**, *12* (Suppl. S1), S41–S45. [[CrossRef](#)]
18. Millonig, G.; Friedrich, S.; Adolf, S.; Fonouni, H.; Golriz, M.; Mehrabi, A.; Stiefel, P.; Poschl, G.; Buchler, M.W.; Seitz, H.K.; et al. Liver stiffness is directly influenced by central venous pressure. *J. Hepatol.* **2010**, *52*, 206–210. [[CrossRef](#)]
19. Millonig, G.; Reimann, F.M.; Friedrich, S.; Fonouni, H.; Mehrabi, A.; Buchler, M.W.; Seitz, H.K.; Mueller, S. Extrahepatic cholestasis increases liver stiffness (FibroScan) irrespective of fibrosis. *Hepatology* **2008**, *48*, 1718–1723. [[CrossRef](#)]
20. Berzigotti, A.; De Gottardi, A.; Vukotic, R.; Siramolpiwat, S.; Abraldes, J.G.; Garcia-Pagan, J.C.; Bosch, J. Effect of meal ingestion on liver stiffness in patients with cirrhosis and portal hypertension. *PLoS ONE* **2013**, *8*, e58742. [[CrossRef](#)]
21. Potthoff, A.; Attia, D.; Pischke, S.; Kirschner, J.; Mederacke, I.; Wedemeyer, H.; Manns, M.P.; Gebel, M.J.; Rifai, K. Influence of different frequencies and insertion depths on the diagnostic accuracy of liver elastography by acoustic radiation force impulse imaging (ARFI). *Eur. J. Radiol.* **2013**, *82*, 1207–1212. [[CrossRef](#)] [[PubMed](#)]
22. Boursier, J.; Cales, P. Clinical interpretation of Fibroscan(R) results: A real challenge. *Liver Int.* **2010**, *30*, 1400–1402. [[CrossRef](#)]
23. Goetze, O.; Breuer, M.; Geier, A.; Fried, M.; Weber, A.; Jochum, W.; Ilan, Y.; Mullan, B. The 13C-methactin breath test is non-inferior to liver biopsy in predicting liver-related death and transplantation: A 7-year prospective follow-up study in 132 patients with chronic hepatitis C infection. *GastroHep* **2020**, *2*, 344–350. [[CrossRef](#)]
24. Ciccocioppo, R.; Candelli, M.; Di Francesco, D.; Ciocca, F.; Taglieri, G.; Armuzzi, A.; Gasbarrini, G.; Gasbarrini, A. Study of liver function in healthy elderly subjects using the 13C-methacetin breath test. *Aliment. Pharmacol. Ther.* **2003**, *17*, 271–277. [[CrossRef](#)] [[PubMed](#)]
25. Pffaffenbach, B.; Gotze, O.; Szymanski, C.; Hagemann, D.; Adamek, R.J. The 13C-methacetin breath test for quantitative noninvasive liver function analysis with an isotope-specific nondispersive infrared spectrometer in liver cirrhosis. *Dtsch. Med. Wochenschr.* **1998**, *123*, 1467–1471. [[CrossRef](#)] [[PubMed](#)]
26. Lalazar, G.; Pappo, O.; Hershovici, T.; Hadjaj, T.; Shubi, M.; Ohana, H.; Hemed, N.; Ilan, Y. A continuous 13C methacetin breath test for noninvasive assessment of intrahepatic inflammation and fibrosis in patients with chronic HCV infection and normal ALT. *J. Viral. Hepat.* **2008**, *15*, 716–728. [[CrossRef](#)]

27. Kochel-Jankowska, A.; Hartleb, M.; Jonderko, K.; Kaminska, M.; Kasicka-Jonderko, A. 13C-methacetin breath test correlates with clinical indices of liver disease severity in patients with primary biliary cirrhosis. *J. Physiol. Pharmacol.* **2013**, *64*, 27–33.
28. Fontana, R.J.; Stravitz, R.T.; Durkalski, V.; Hanje, J.; Hameed, B.; Koch, D.; Reuben, A.; Ganger, D.; Olson, J.; Liou, I.; et al. Prognostic Value of the (13) C-Methacetin Breath Test in Adults with Acute Liver Failure and Non-acetaminophen Acute Liver Injury. *Hepatology* **2021**, *74*, 961–972. [[CrossRef](#)]
29. Vranova, J.; Hendrichova, M.; Kolarova, H.; Kratka, K.; Rosina, J.; Horak, J. (1)(3)C-methacetin breath test in the evaluation of disease severity in patients with liver cirrhosis. *Biomed. Pap. Med. Fac. Univ. Palacky Olomouc Czech Repub.* **2013**, *157*, 392–400. [[CrossRef](#)]
30. Mueller, S.; Sandrin, L. Liver stiffness: A novel parameter for the diagnosis of liver disease. *Hepat. Med.* **2010**, *2*, 49–67. [[CrossRef](#)]
31. Belloni, A.; Chernozhukov, V.; Hansen, C. Inference in High-Dimensional Panel Models With an Application to Gun Control. *J. Bus. Econ. Stat.* **2016**, *34*, 590–605. [[CrossRef](#)]
32. Lane, E.A.; Parashos, I. Drug pharmacokinetics and the carbon dioxide breath test. *J. Pharmacokinet. Biopharm.* **1986**, *14*, 29–49. [[CrossRef](#)] [[PubMed](#)]
33. Brunger, A.F.; van Rheenen, R.; Gans, R.O.B.; Hazenberg, B.P.C.; Nienhuis, H.L.A. How well does liver span as part of the consensus criteria for liver involvement in AL amyloidosis perform? *Amyloid* **2023**, *30*, 437–439. [[CrossRef](#)] [[PubMed](#)]
34. Malek, F.; Hendrichova, M.; Kratka, K.; Sedlakova, M.; Vranova, J.; Horak, J. Correlation of the functional liver mass with left ventricular ejection fraction and left atrial diameter in patients with congestive heart failure. *Int. J. Cardiol.* **2008**, *127*, 271–273. [[CrossRef](#)] [[PubMed](#)]
35. Hendrichova, M.; Malek, F.; Koprivova, H.; Vranova, J.; Ostadal, P.; Kratka, K.; Sedlakova, M.; Horak, J. Correlation of NT-proBNP with metabolic liver function as assessed with (13)C-methacetin breath test in patients with acute decompensated heart failure. *Int. J. Cardiol.* **2010**, *144*, 321–322. [[CrossRef](#)] [[PubMed](#)]
36. Law, S.; Petrie, A.; Chacko, L.; Cohen, O.C.; Ravichandran, S.; Gilbertson, J.A.; Rowczenio, D.; Wechalekar, A.; Martinez-Naharro, A.; Lachmann, H.J.; et al. Disease progression in cardiac transthyretin amyloidosis is indicated by serial calculation of National Amyloidosis Centre transthyretin amyloidosis stage. *ESC Heart Fail.* **2020**, *7*, 3942–3949. [[CrossRef](#)]
37. Palladini, G.; Lavatelli, F.; Russo, P.; Perlini, S.; Perfetti, V.; Bosoni, T.; Obici, L.; Bradwell, A.R.; D’Eril, G.M.; Fogari, R.; et al. Circulating amyloidogenic free light chains and serum N-terminal natriuretic peptide type B decrease simultaneously in association with improvement of survival in AL. *Blood* **2006**, *107*, 3854–3858. [[CrossRef](#)] [[PubMed](#)]
38. Cheng, R.K.; Levy, W.C.; Vasbinder, A.; Teruya, S.; De Los Santos, J.; Leedy, D.; Maurer, M.S. Diuretic Dose and NYHA Functional Class Are Independent Predictors of Mortality in Patients With Transthyretin Cardiac Amyloidosis. *JACC CardioOncol* **2020**, *2*, 414–424. [[CrossRef](#)]
39. Brons, M.; Muller, S.A.; Rutten, F.H.; van der Meer, M.G.; Vrancken, A.; Minnema, M.C.; Baas, A.F.; Asselbergs, F.W.; Oerlemans, M. Evaluation of the cardiac amyloidosis clinical pathway implementation: A real-world experience. *Eur. Heart J. Open* **2022**, *2*, oeac011. [[CrossRef](#)]
40. Tini, G.; Milani, P.; Zampieri, M.; Caponetti, A.G.; Fabris, F.; Foli, A.; Argiro, A.; Mazzoni, C.; Gagliardi, C.; Longhi, S.; et al. Diagnostic pathways to wild-type transthyretin amyloid cardiomyopathy: A multicentre network study. *Eur. J. Heart Fail.* **2023**, *25*, 845–853. [[CrossRef](#)]

**Disclaimer/Publisher’s Note:** The statements, opinions and data contained in all publications are solely those of the individual author(s) and contributor(s) and not of MDPI and/or the editor(s). MDPI and/or the editor(s) disclaim responsibility for any injury to people or property resulting from any ideas, methods, instructions or products referred to in the content.